Evaluation of Various Types of Wall Boundary Conditions for the Boltzmann Equation

Christopher D. Wilson[a], Ramesh K. Agarwal[a], and Felix G. Tcheremissine[b]

[a]*Department of Mechanical Engineering and Materials Science*
Washington University in St. Louis, Missouri 63130, USA

[b]*Mechanics Department*
Computing Center of Academy of Science, Moscow, Russia

Abstract. This paper presents the evaluation of several solid wall boundary conditions when used in the numerical solution of the Boltzmann equation using the finite-difference/finite-volume methods. Five solid wall boundary conditions are considered: (a) adsorption, (b) specular reflection, (c) diffuse reflection, (d) Maxwellian reflection, and (e) adsorptive Maxwellian reflection. The boundary conditions are applied on a two-dimensional discretized velocity space mesh. Methods for applying the same boundary conditions on a three-dimensional velocity space grid are also presented. The boundary conditions are implemented for the numerical solution of the hypersonic rarefied flow over a flat plate using a three-dimensional generalized Boltzmann equation (GBE) solver. The derivatives that contribute to heat transfer and skin friction at the solid boundary are calculated and compared. Recommendations for further evaluation of the boundary conditions are made.

Keywords: Boltzmann Equation, Boundary Conditions, Hypersonic Flow, Flat Plate
PACS: 51.10.+y, 05.20.Dd

INTRODUCTION

Application of appropriate boundary conditions in the computational domain is crucial to obtaining accurate solutions for any problem being solved analytically or numerically. Appropriate types of boundary conditions must be implemented on various boundaries of the computational domain. The various types of boundary conditions, and where they are applied in the computational domain, are discussed in the following sections. The main emphasis is placed on the solid wall boundary conditions. Five types of boundary conditions: (a) adsorptive, (b) specular reflection, (c) diffuse reflection, (d) Maxwellian reflection, and (e) adsorptive Maxwellian reflection are considered, implemented, and evaluated for their accuracy in computing the skin friction and heat transfer on the solid wall.

INFLOW BOUNDARY CONDITION

The inflow boundary condition is assumed to be a Dirichlet boundary condition. It is assumed that the inflow boundary is at equilibrium. A Maxwellian distribution function centered at the mean velocity of the incoming flow is used at all the grid points of the inflow boundary. This condition is maintained at each time step. An example of the inflow boundary condition using the Maxwellian distribution function is shown on the left side (L) of Figure 1.

SOLID WALL BOUNDARY CONDITIONS

Five solid wall boundary conditions are considered for application to the problem of flow around immersed bodies – adsorption, specular reflection, diffuse reflection, Maxwellian reflection, and adsorptive Maxwellian reflection. These boundary conditions range from relatively simple to implement to difficult to implement, and from

physically unrealistic to requiring tuning of the accommodation coefficient to match the empirical data. The formulation of each of these boundary conditions and their implementation are discussed in the following sections.

Adsorption

The adsorptive boundary condition is analogous to the no slip boundary condition for viscous walls in continuum solvers. Adsorption needs to be accompanied by a de-adsorptive phase in order for the conservation of mass to be satisfied at the solid wall boundary. An approach for modeling adsorption/de-adsorption at the wall is to apply a Maxwellian distribution centered at zero velocity using the probability densities from the physical space grid point at the preceding time step. This approach to the adsorptive boundary condition, as applied in a two-dimensional velocity space is illustrated in the right hand side (R) of Figure 1. The inflow boundary condition is also depicted with the adsorptive boundary condition for reference. The adsorptive boundary condition is independent of the angle of incidence of the surface relative to the incoming flow. Application of this method to a three-dimensional velocity space simply involves utilizing the Maxwellian distribution that is a function of the three coordinate direction velocities.

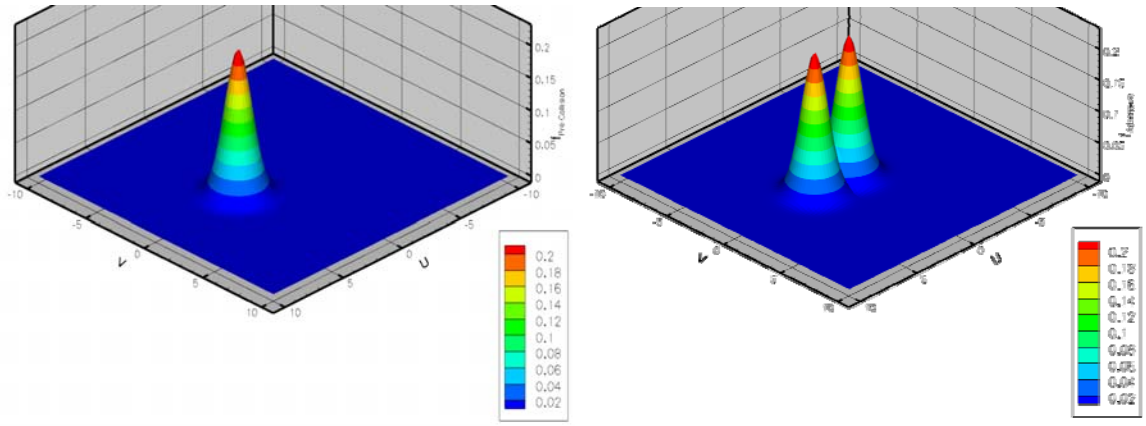

FIGURE 1. Inflow boundary condition (L) and adsorptive boundary condition (R)

Specular Reflection

The specular reflection boundary condition implies that molecules reflect off of the solid wall with the angles of incidence and reflection being equal. A fundamental assumption behind specular reflection is a completely smooth surface. Making that assumption is not completely realistic when simulating molecular interactions with a real surface. The magnitude of the velocity after the collision is the same as the velocity before the collision. However, the component of the velocity vector normal to the surface changes sign. The normal vector, $\hat{n}$ of the solid wall needs to be calculated at each physical space node. Then the reflected velocity, $\vec{\xi}_r$ can be related to the incident velocity, $\vec{\xi}_i$, using Equation (1). The probability for each point in the reflected velocity space is calculated using weighted area interpolation for a two-dimensional velocity space, using Equation (2), or weighted volume interpolation for a three-dimensional velocity space. The relationship between the areas, *A*, and the probabilities, *f*, are shown in Figure 2. The interpolated probability value is then transferred to the reflected velocity space grid point using Equation (3). The results of applying the specular reflection boundary condition in a two-dimensional velocity space for two angles of incidence (90° and 0°) are shown in Figures 3.

$$\vec{\xi}_i = \vec{\xi}_r - 2\hat{n}\left(\vec{\xi}_r \cdot \hat{n}\right) \text{ for } \vec{\xi}_r \cdot \hat{n} \geq 0 \tag{1}$$

$$f_i\left(\vec{\xi}_i\right) = \frac{1}{A}\left(A_{m,n} f_{m,n} + A_{m,n+1} f_{m,n+1} + A_{m+1,n} f_{m+1,n} + A_{m+1,n+1} f_{m+1,n+1}\right) \tag{2}$$

$$f_r\left(\vec{\xi}_r\right) = f_i\left(\vec{\xi}_i\right) \tag{3}$$

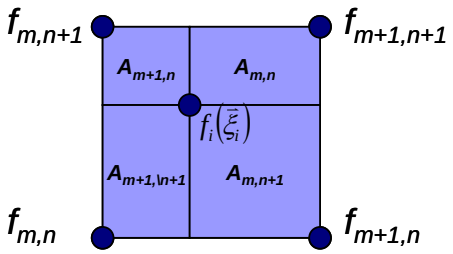

FIGURE 2. Weighted area average for incident molecule probability undergoing specular reflection

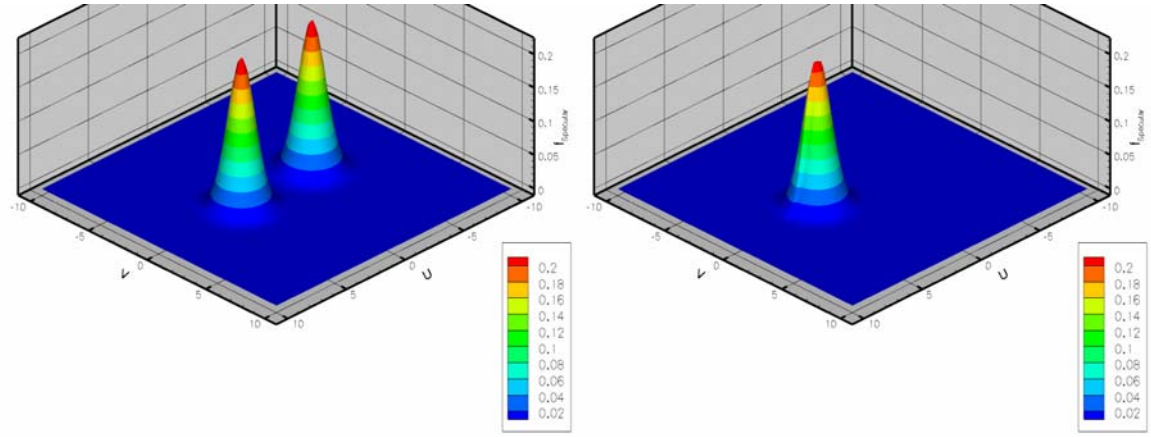

FIGURE 3. Specular reflection boundary condition for incidence angles of 90° (L) and 0°(R)

The solid wall boundary surface can be visualized as a plane within the three-dimensional velocity space that intersects the origin and is perpendicular to the surface normal. In these two-dimensional representations, the plane collapses to a line that lies within the *uv* plane. Again, the line runs directly through the origin of velocity space. These figures illustrate that the distribution function contained in the velocity space domain that is located in the direction opposite the surface normal is reflected across the plane (or line) that defines the surface boundary into the domain of velocity space that is located in the direction of the surface normal. For the surface perpendicular to the incoming flow, almost all of the distribution function is reflected into the upwind part of the velocity space domain. At an incidence angle of 0° (a surface parallel to the incoming flow) only half of the distribution function is reflected, essentially reproducing the inflow distribution function. The specular reflection boundary condition is equivalent to an inviscid wall in a continuum flow solver.

Diffuse Reflection

The diffuse reflection boundary condition is a better approximation of the seemingly random interaction of molecules with a rough surface. The diffuse reflection can be modeled by using uniformly distributed set of random numbers to vary the velocity of the reflected particle. The molecular speed values can be generated using the cumulative distribution function, as presented by Shen [1], shown in Equation (4). In Equation (4), $\vec{\xi}_r$ is the reflected velocity, k is the Boltzmann constant, m is the molecular mass, T_r is the temperature of the molecule undergoing the reflection, and *ranf* is a random fraction uniformly distributed between zero and one. For a two-dimensional velocity space, the scattering direction, θ, is determined from a uniformly distributed random number between zero and π, as shown in Equation (5). For a three-dimensional velocity space, the scattering direction in the plane parallel to the surface, ϕ, also needs to be considered. The pre-collision probabilities are incrementally distributed to the reflected velocity space grid using a similar weighted area (or volume) approach as for the specular reflection. A total probability for each reflected velocity space grid point is determined by summing all of the incremental contributions.

$$\left|\vec{\xi}_r\right| = \frac{1}{\beta}\sqrt{-\ln(ranf)} \text{ where } 0 \le ranf < 1 \text{ and } \beta = \left(2\frac{k}{m}T_r\right)^{-1/2} \tag{4}$$

$$\theta = \pi \cdot ranf \text{ where } 0 \le ranf < 1 \text{ and } \phi = 2\pi \cdot ranf \text{ where } 0 \le ranf < 1 \tag{5}$$

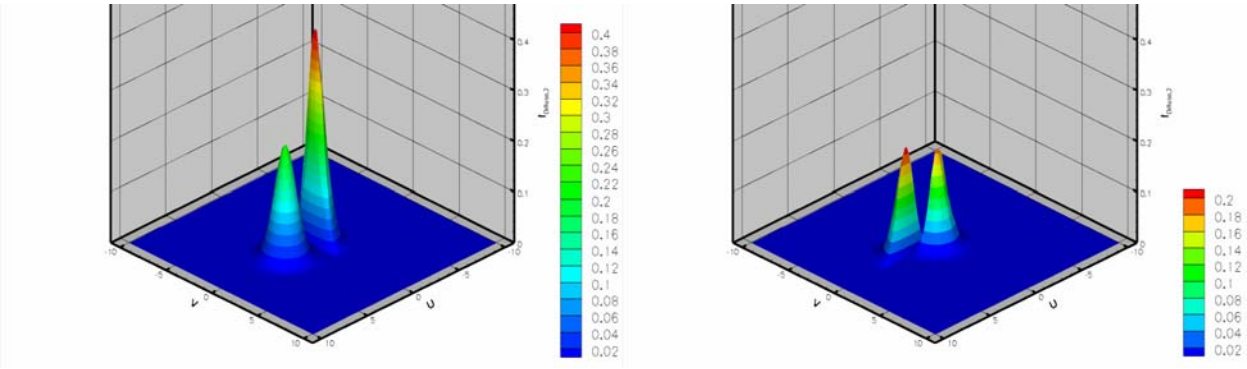

FIGURE 4. Diffuse reflection boundary condition for incidence angles of 90° (L) and 0° (R)

The surface is defined in the same manner as for the specular reflection. Therefore, the scattering direction is defined by an angle relative to the surface normal vector. For the case where the surface is perpendicular to the incoming flow, the entire distribution function is reflected and scattered into the part of the velocity space domain that lies in the direction of the surface normal. Unlike the specular reflection, the distribution function for the diffuse reflection has the highest probability for a velocity located at the origin of velocity space. The total probability density for the inflow distribution function and the diffusely reflected distribution function are equal. When the angle of incidence reaches 0°, only half of the inflow distribution function is reflected at the boundary. Again, the total probability density for the inflow distribution is the same as the diffusely reflected distribution function.

Maxwellian Reflection

The Maxwellian boundary condition is a combination of specular and diffuse reflection. It is assumed that a certain percentage of incident molecules undergo specular reflection. The remaining proportion of molecules undergoes diffuse reflection. The percentage of molecules that undergo diffuse reflection is called the accommodation coefficient, α. The resulting probability distribution is determined using Equation (6). The accommodation coefficient, α, can be adjusted to empirically match experimental data to accurately reflect differences in surface properties. The results of applying the Maxwellian reflection boundary condition in a two-dimensional velocity space are shown in Figure 5. The value of the accommodation coefficient, α, is equal to 0.5.

$$f_{Maxwellian} = \alpha f_{Diffuse} + (1-\alpha) f_{Specular} \tag{6}$$

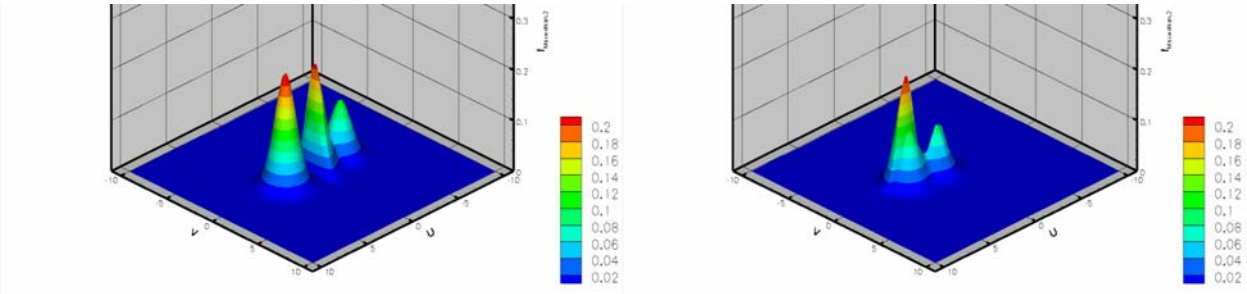

FIGURE 5. Maxwellian reflection boundary condition (α = 0.5) for incidence angles of 90° (L) and 0° (R)

The Maxwellian distribution, for an accommodation coefficient equal to 0.5, results in half of the specular reflection boundary condition and half of the diffuse reflection boundary condition being represented in the part of the velocity space domain located in the direction of the surface normal. For an incidence angle equal to 90°, the diffuse reflection component appears to be of the same magnitude as the inflow distribution function, but only half of the distribution is present (the half that is in the direction of the surface normal). The specular reflection component appears to be comprised of a complete Maxwellian distribution, but the magnitudes are one half of the inflow values. The diffuse reflection probabilities become less dominant over the specular reflection probabilities as the angle of incidence reaches zero. These observations may change if a different accommodation coefficient is selected. If either zero or one are selected, then the observations would be the same as for the specular reflection or the diffuse reflection, respectively.

Adsorptive Maxwellian Reflection

The last boundary condition is a combination of adsorption and Maxwellian reflection. A new coefficient, β, is introduced to represent the proportion of molecules that experience adsorption. The remaining molecules are assumed to experience the Maxwellian reflection, which is distributed between specular and diffuse reflections according to the selected accommodation coefficient, α. The probability distribution function is determined using Equation (7). The results of applying the adsorptive Maxwellian boundary condition in a two-dimensional velocity space for various incident angles are shown in Figure 6. The two coefficients, α and β, are equal to 0.5 and 0.33, respectively. As a result, the probability distribution function is comprised of equal parts of adsorption, specular reflection, and diffuse reflection.

$$f_{Adsorptive-Maxwellian} = \beta f_{Adsorptive} + (1-\beta)\left(\alpha f_{Diffuse} + (1-\alpha) f_{Specular}\right) \tag{7}$$

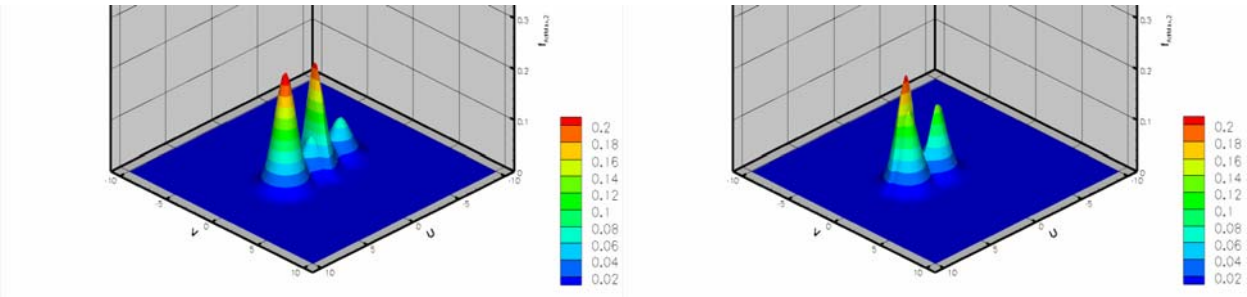

FIGURE 6. Adsorptive Maxwellian reflection boundary condition (α = 0.5, β = 0.33) for incidence angles of 90° and 0°

It is clear by examining Figure 6 that the probabilities associated with the specular reflection component are reduced beyond that of the Maxwellian reflection. The magnitude of the diffuse reflection component located at the origin of the velocity space appears unchanged. This appearance is due to the fact that the adsorptive boundary condition, also located at the origin of the velocity space, now comprises part of the reflected boundary condition. It is important to note that the behavior noted in the preceding discussion will undoubtedly change if different values for α and β are chosen.

APPLICATION OF BOUNDARY CONDITIONS TO FLOW OVER A FLAT PLATE

The solid wall boundary conditions discussed in the preceding sections were applied to simulation of supersonic flow over a flat plate, at Mach 3, using a direct Boltzmann solver based on the approach of Tcheremissine [2]. These simulations were conducted in order to make a preliminary determination regarding the effectiveness of each type of boundary condition in simulating the flow near a solid wall boundary. The equivalent Knudsen number is 0.5 since the flat plate extends between 4.0 and 6.0 in the X/λ direction. A wall temperature equal to the freestream value was assumed for the adsorptive boundary condition. An example of the Mach number and density contours is shown for the diffuse reflection boundary condition in Figure 7. The five boundary conditions can be compared by calculating the partial derivatives that are proportional to skin friction and heat transfer, as shown in Equation (8). Figure 8 presents a comparison of the skin friction and heat transfer properties along the surface of the flat plate.

$$c_f \propto \frac{\partial(U/U_\infty)}{\partial(Z/\lambda)} \text{ and } q \propto \frac{\partial(T/T_\infty)}{\partial(Z/\lambda)} \tag{8}$$

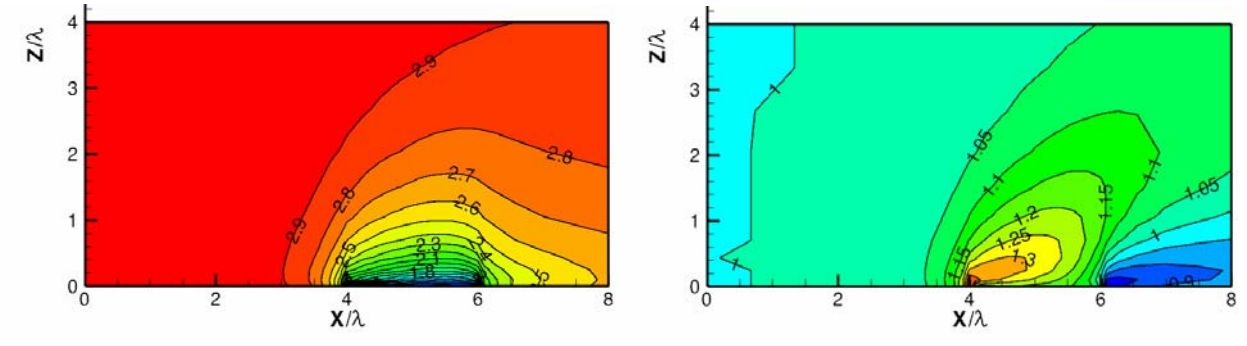

FIGURE 7. Mach number and density contours for diffuse reflection along a flat plate at Mach 3

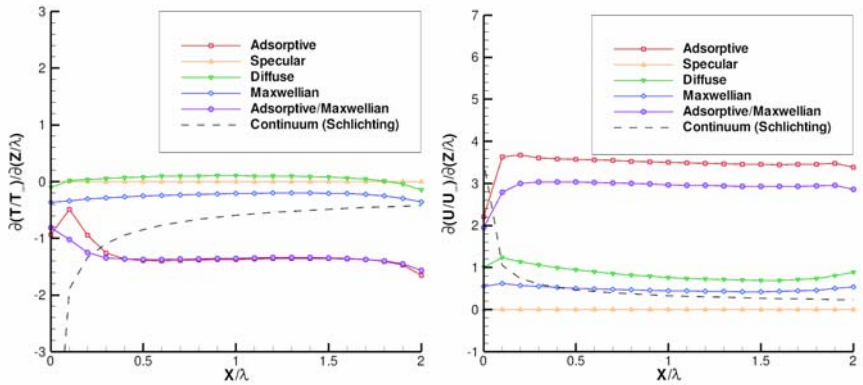

FIGURE 8. Comparison of derivative for skin friction and heat transfer for flow along a flat plate at Mach 3

As expected, the heat transfer and skin friction for the specular reflection boundary condition is zero across the entire surface of the flat plate. The diffuse reflection boundary condition results in heat transfer values that are not too dissimilar from the specular reflection values. However, the skin friction values are higher for diffuse reflection. For the Maxwellian reflection, the skin friction falls between the values obtained for specular reflection and the diffuse reflection. Interestingly, the Maxwellian reflection results in absolute values of heat transfer that are higher than those obtained from either specular reflection or diffuse reflection. The adsorptive boundary condition yields the highest skin friction values and the highest absolute heat transfer values. When combined with the Maxwellian reflection, the adsorptive boundary condition dominates the heat transfer process and results in a profile that is almost the same as pure adsorption. The adsorptive boundary condition also dominates the skin friction values, but to a lesser extent.

SUMMARY

For simulating flow over a flat plate, pure adsorption results in the highest values of skin friction and heat transfer. Pure specular reflection results in the lowest values of skin friction and heat transfer. Diffuse reflection results in skin friction values that fall between the adsorptive and specular reflection values. The Maxwellian reflection yields some flexibility in tuning the skin friction and heat transfer values across the plate. However, combining the adsorptive boundary with the Maxwellian reflection enables an even greater degree of flexibility. This flexibility will be extraordinarily useful when attempting to match numerical simulations to experimental data.

REFERENCES

1. C. Shen, *Rarefied Gas Dynamics: Fundamentals, Simulations & Micro Flows*, Springer-Verlag, Berlin, 2005.
2. F. G. Tcheremissine, *Doklady Physics* **47**, 872-875 (2002).